

Are your **MRI contrast agents** cost-effective?

Learn more about generic **Gadolinium-Based Contrast Agents**.



**AJNR**

**Diffusion-Weighted and Conventional MR  
Imaging Findings of Neuroaxonal Dystrophy**

R. Nuri Sener

*AJNR Am J Neuroradiol* 2004, 25 (7) 1269-1273

<http://www.ajnr.org/content/25/7/1269>

This information is current as  
of April 17, 2024.

# Diffusion-Weighted and Conventional MR Imaging Findings of Neuroaxonal Dystrophy

R. Nuri Sener

**BACKGROUND AND PURPOSE:** Neuroaxonal dystrophy is a rare progressive disorder of childhood characterized by mental deterioration and seizures. The diffusion-weighted and conventional MR imaging findings are reported for six cases.

**METHODS:** Six patients aged 19 months to 9 years with proved neuroaxonal dystrophy (one with the infantile form, five juvenile forms) underwent imaging at 1.5 T. Echo-planar diffusion-weighted images were acquired with a trace imaging sequence in five patients and with a three-gradient protocol (4000/110) in one. Images obtained with a  $b$  value of  $1000 \text{ s/mm}^2$  and corresponding apparent diffusion coefficient (ADC) maps were studied. ADCs from lesion sites and normal regions (pons and temporal and occipital lobes) were evaluated.

**RESULTS:** A hyperintense cerebellum (a characteristic of the disease) was evident on fluid-attenuated inversion recovery images in all cases. Four patients had associated cerebral changes. Diffusion-weighted images, especially ADC maps, showed an elevated diffusion pattern in the cerebellum in the five juvenile cases (normal images at  $b = 1000 \text{ s/mm}^2$ , ADCs of  $1.30\text{--}2.60 \times 10^{-3} \text{ mm}^2/\text{s}$ ). A restricted diffusion pattern was evident in the infantile case (hyperintensity at  $b = 1000 \text{ s/mm}^2$ , low ADCs of  $0.44\text{--}0.55 \times 10^{-3} \text{ mm}^2/\text{s}$ ). ADCs were normal in the pons and temporal and occipital lobes ( $0.64\text{--}1.00 \times 10^{-3} \text{ mm}^2/\text{s}$ ).

**CONCLUSION:** An elevated cerebellar diffusion pattern is a predominant feature of juvenile neuroaxonal dystrophy. Coexistent elevated and restricted diffusion patterns were evident in different brain regions in different forms of the disease. Dystrophic axons likely account the restricted diffusion, whereas spheroid formation (swelling) and abnormal myelination result in elevated diffusion.

Neuroaxonal dystrophy is a rare progressive disorder of childhood characterized by mental deterioration and seizures. It is also characterized by the widespread presence of dystrophic axons in both the central nervous system and the peripheral nervous system (1–7). The disorder consists of mainly infantile, juvenile, and adult forms. It was previously described by means of MR imaging (1–6), and its diffusion MR imaging findings are discussed in one report (7). Hyperintensity in the cerebellar cortex on T2-weighted images is the most characteristic MR imaging finding (1–6) and is best appreciated on fluid-attenuated inversion recovery (FLAIR) images (7).

The purpose of this study was to investigate the diffusion-weighted and conventional MR imaging findings in six cases of neuroaxonal dystrophy: one

with the infantile form of the disease and five with the juvenile form.

## Methods

Six patients had proved neuroaxonal dystrophy established by means of biopsy of the terminal motor fibers in the lower extremity that revealed dystrophic nerve fibers. Denervation of the lower extremities was noted during electromyography in each patient. The patients included three boys and three girls, two of whom were siblings. The patients were aged 19 months to 9 years. The 19-month-old male patient had the infantile form of the disease. The two female siblings (5 and 9 years old), a 6-year-old boy, a 5-year-old boy, and a 5-year-old girl had the juvenile form of the disease. Rigidity of the extremities, progressive deterioration of motor function, and difficulty with or loss of speech were common symptoms in the patients.

MR imaging was performed with 1.5-T systems (Magnetom Vision or Symphony; Siemens, Erlangen, Germany). Conventional spin-echo T1- and T2-weighted images, including FLAIR images, were obtained in all patients. Five underwent echo-planar diffusion-weighted MR imaging with a trace imaging sequence (TR/TE = 5700/139). One patient (a 19-month-old boy) was imaged with an echo-planar three-gradient protocol (4000/110). Images obtained at a  $b$  value of  $1000 \text{ s/mm}^2$  and automatically generated apparent diffusion coefficient (ADC) maps were studied. ADC values were calculated by using electronic readings from ADC maps. Evaluations of

Received September 10, 2003; accepted after revision December 22.

From the Department of Radiology, Ege University Hospital, Bornova, Izmir, Turkey.

Address reprint requests to Prof. Dr R. Nuri Sener, Department of Radiology, Ege University Hospital, Bornova, Izmir, 35100, Turkey.

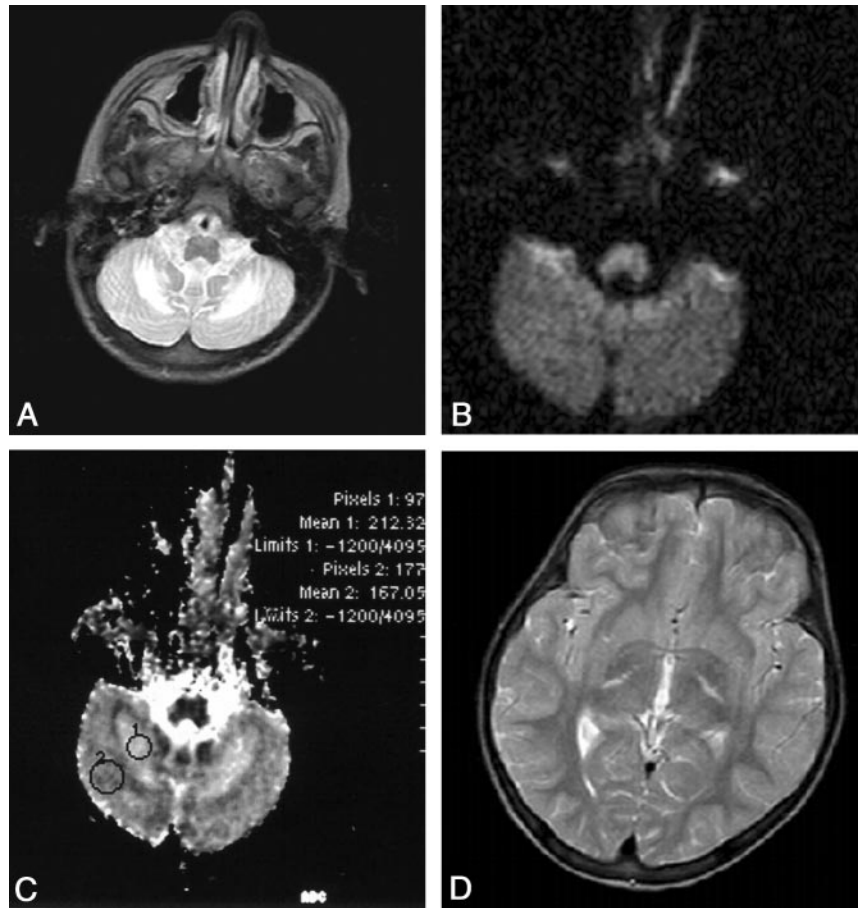
FIG 1. Images obtained in a 5-year-old girl. (Her sibling, a 9-year-old girl, was similarly affected.)

A, T2-weighted image reveals characteristic hyperintensity of the cerebellum. The dentate nuclei have higher signal intensity.

B, Diffusion-weighted image obtained at a  $b$  value of  $1000 \text{ s/mm}^2$  appears normal.

C, ADC map (section identical to that in B) is abnormal. ADC values in the cerebellum are high and higher in the dentate nuclei ( $2.12 \times 10^{-3} \text{ mm}^2/\text{s}$ ) than the surrounding parenchyma ( $1.67 \times 10^{-3} \text{ mm}^2/\text{s}$ ); these all indicate elevated diffusion rates.

D, T2-weighted image reveals hyperintense lesions in the corticospinal tract.



variably sized circular regions of interest and pixel-lens evaluations (6 pixels) were conducted. Values from the lesion sites and normal brain regions (pons and temporal and occipital lobes) were assessed.

## Results

In all the patients, the cerebellum showed atrophy, as evidenced by prominent folia. Hyperintensity of the cerebellum was evident on T2-weighted and FLAIR images; this finding is a characteristic feature of the disease (Figs 1–5). In addition, images in four patients demonstrated changes in the supratentorial region. These included hyperintense lesions in the posterior limbs of the internal capsules (in the corticospinal tracts) in the two siblings (Fig 1). In another patient, hyperintense lesions were confined to the genu and splenium of the corpus callosum (Fig 2). Another had hyperintense changes in the vicinity of the frontal horns of the lateral ventricles. In the remaining two patients, there was no apparent supratentorial lesion. The findings are summarized in the Table.

With respect to the diffusion MR imaging findings in the cerebellum, images obtained at a  $b$  value of  $1000 \text{ s/mm}^2$  appeared normal in the five patients with the juvenile form of the disease (Fig 1B). Their ADC maps revealed high signal intensity and increased

ADC values in the cerebellar parenchyma compared with values in normal regions of the brain (ADC values from the pons and temporal and occipital lobes were  $0.64\text{--}1.00 \times 10^{-3} \text{ mm}^2/\text{s}$ ). Therefore, in these five juvenile cases, an elevated diffusion pattern manifested normal-appearing images at the  $b$  value of  $1000 \text{ s/mm}^2$  and high ADC values of  $1.30\text{--}2.60 \times 10^{-3} \text{ mm}^2/\text{s}$ . Of note, ADC maps revealed that the cerebellar cortex and also the medullary regions surrounding the dentate nuclei were involved (Figs 1–5). In the female siblings, the dentate nuclei were also involved, and the ADC values were higher than those of the surrounding cerebellar parenchyma (Fig 1). In the 19-month-old male patient with the infantile form of the disease, a restricted diffusion pattern was evident. This pattern consisted of hyperintense changes involving the folia on images obtained at a  $b$  value of  $1000 \text{ s/mm}^2$  and images associated with low ADC values ( $0.44\text{--}0.55 \times 10^{-3} \text{ mm}^2/\text{s}$ ) (Fig 2). With respect to the supratentorial changes, high signal intensity on images obtained at a  $b$  value of  $1000 \text{ s/mm}^2$  was associated with low ADC values (restricted diffusion) in three patients (the two female siblings and the 19-month-old male patient) (Figs 1 and 2). In one patient, images obtained at a  $b$  value of  $1000 \text{ s/mm}^2$  appeared normal, whereas ADC maps revealed high ADC values (elevated diffusion) (Fig 3, Table).

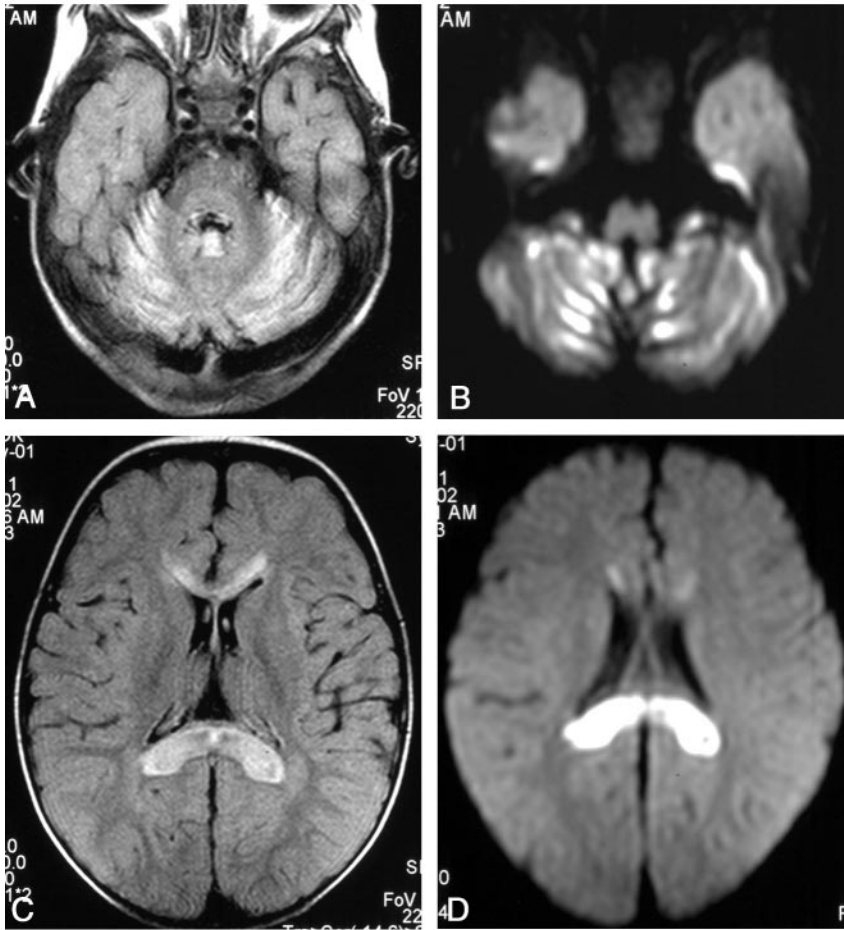


FIG 2. Images obtained in a 19-month-old male patient.

A, FLAIR image reveals characteristic hyperintensity of the cerebellum.

B, Diffusion-weighted image obtained at a  $b$  value of  $1000 \text{ s/mm}^2$  reveals hyperintensities in the folia (restricted diffusion).

C, FLAIR image reveals hyperintensities in the genu and splenium of the corpus callosum.

D, Diffusion-weighted image obtained at a  $b$  value of  $1000 \text{ s/mm}^2$  reveals hyperintensity of the splenium, indicating restricted diffusion. (The genu was similarly involved.)

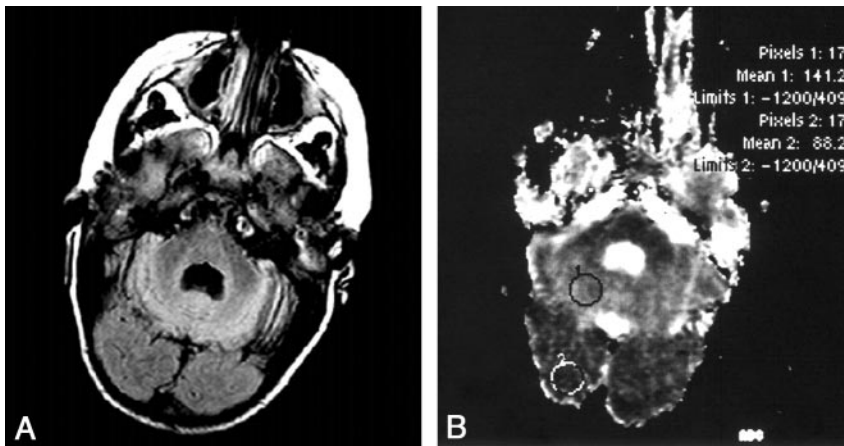


FIG 3. Image obtained in a 6-year-old boy.

A, FLAIR image reveals characteristic hyperintensity of the cerebellum.

B, ADC map reveals an increased ADC value ( $1.41 \times 10^{-3} \text{ mm}^2/\text{s}$ ) in the cerebellum, indicating elevated diffusion compared with a normal ADC value ( $0.88 \times 10^{-3} \text{ mm}^2/\text{s}$ ) in the occipital lobe. (Diffusion-weighted image obtained at a  $b$  value of  $1000 \text{ s/mm}^2$  appeared normal.)

### Discussion

Patients with neuroaxonal dystrophy can present with sporadic or familial cases. The juvenile form of the disease is mostly sporadic, with a slightly higher incidence in girls in the reported patients, and the familial cases have a 2:1 female preponderance (1–6). This study included two female siblings with the familial disease, and the remaining four patients had sporadic cases.

With respect to histopathologic traits of neuroaxonal dystrophy, the most characteristic microscopic features are cerebellar atrophy, widespread spheroid

formation, and abnormal myelin patterns. Swollen, dystrophic axons are present in both the central nervous system and the peripheral nervous system (6). Diffusion-weighted MR imaging can be expected to reflect these histopathologic changes, when prominent.

A previous case report described changes depicted by diffusion-weighted MR imaging in the infantile form of neuroaxonal dystrophy (7). The patient was a 7-month-old female infant, and MR imaging revealed mainly diffuse atrophy, diminished myelination, and hyperintensity of the cerebellar cortex. The pyramidal

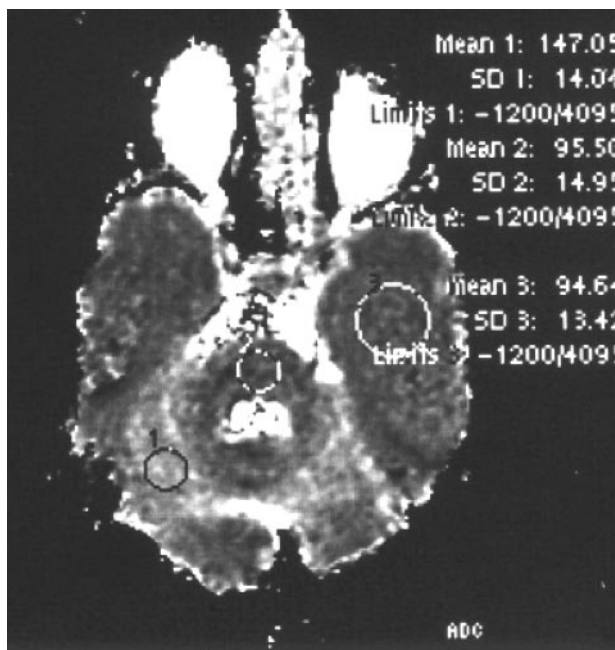


FIG 4. Images obtained in a 5-year-old boy. ADC map reveals an increased ADC value ( $1.47 \times 10^{-3} \text{ mm}^2/\text{s}$ ) in the cerebellum compared with normal values from the pons ( $0.95 \times 10^{-3} \text{ mm}^2/\text{s}$ ) and temporal lobe ( $0.94 \times 10^{-3} \text{ mm}^2/\text{s}$ ).

tract and dentate nuclei had high signal intensity on diffusion-weighted images occurred at a  $b$  value of  $1000 \text{ s/mm}^2$  and low ADC values. The authors suggested that this pattern likely reflected the presence of dystrophic axons with restricted mobility of water molecules. A reverse pattern was evident in the cerebellar cortex, with high ADC values; this was likely a reflection of demyelination or lack of myelination (7). Cerebellar hyperintensity on FLAIR images, which is the most consistent finding of neuroaxonal dystrophies, was present in all six patients in this study (Figs 1–5).

The diffusion-weighted imaging findings in the cerebellum of the five patients with the juvenile form of the disease were similar: normal findings were depicted on images obtained at a  $b$  value of  $1000 \text{ s/mm}^2$  and high ADC values, which corresponded to an elevated diffusion pattern (Figs 1, 3–5). This observation differs from that of a previously published case

report (7). In addition, in the two siblings with the juvenile form, the dentate nuclei had ADC values higher than those of the remaining parenchyma (Fig 1); this fractional elevated diffusion pattern, too, was the opposite to the previous finding that the dentate nuclei have high signal intensity (restricted diffusion) on images obtained at the  $b$  value of  $1000 \text{ s/mm}^2$  (and low ADC values) (7). Only the 19-month-old boy with the infantile form had similar hyperintense changes on images obtained at the  $b$  value of  $1000 \text{ s/mm}^2$  (restricted diffusion); these findings were confined to the folia (Fig 2). Therefore, an elevated diffusion pattern was predominant in the juvenile cases, and a restricted diffusion pattern was evident in a single case of the infantile form. The reason for this difference is unknown. The presence of dystrophic axons likely accounted for restricted diffusion, whereas spheroid formation (swelling) and abnormal myelination resulted in elevated diffusion.

With respect to the cerebral changes, the previous case report presented findings of high signal intensity in the corticospinal tracts on images obtained at a  $b$  value of  $1000 \text{ s/mm}^2$  and low ADC values, which likely reflected the presence of dystrophic axons with restricted mobility of water molecules (7). In the current study, high-signal-intensity changes on images obtained at a  $b$  value of  $1000 \text{ s/mm}^2$  (with low ADC values) were noted in three patients (two juvenile cases, one infantile case) in the cerebrum; this represented a restricted diffusion pattern. Also noted was involvement of the pyramidal tract and the genu and splenium of the corpus callosum. In one patient (juvenile case) with lesions in the deep frontal white matter, an elevated diffusion pattern was evident. These findings likely corresponded to different stages of histopathologic changes.

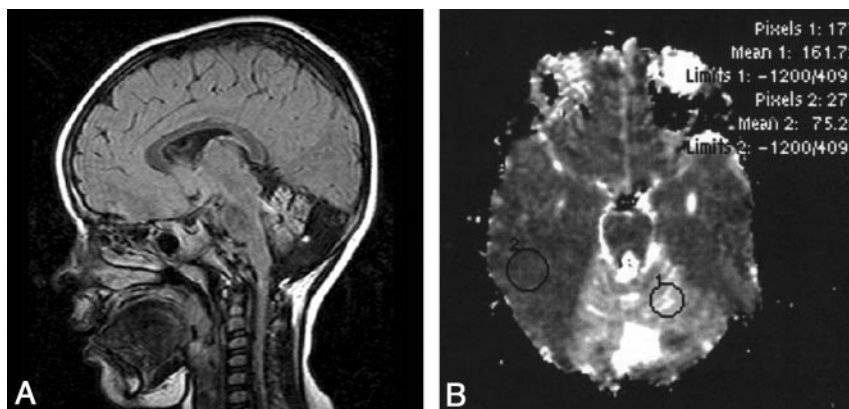
## Conclusion

In all six patients with neuroaxonal dystrophy—one with the infantile form and five with the juvenile form—FLAIR images showed a hyperintense cerebellum, a consistent feature of the disease. Four patients had associated cerebral changes. Diffusion-weighted images ( $b = 1000 \text{ s/mm}^2$ ) and ADC maps in particular provided additional information. In the

FIG 5. Images obtained in a 5-year-old girl.

A, Sagittal FLAIR image reveals characteristic hyperintensity of the vermis.

B, ADC map reveals an increased ADC value in the cerebellum ( $1.61 \times 10^{-3} \text{ mm}^2/\text{s}$ ) compared with the normal value from the right temporal lobe ( $0.75 \times 10^{-3} \text{ mm}^2/\text{s}$ ).



## MR imaging and diffusion MR findings in six patients with neuroaxonal dystrophy

Patient Age/Sex	MRI Supratentorial Changes	Cerebellar Diffusion Imaging		Cerebral Diffusion Imaging	
		$b = 1000$ s/mm <sup>2</sup>	ADC Map	$b = 1000$ s/mm <sup>2</sup>	ADC Map
5 y/F	Corticospinal tract	Normal	High ADC	Hyperintense	Low ADC
9 y/F	Corticospinal tract	Normal	High ADC	Hyperintense	Low ADC
19 mo/M	Corpus callosum genu and splenium	Hyperintense	Low ADC	Hyperintense	Low ADC
6 y/M	Deep white matter, frontal	Normal	High ADC	Normal	High ADC
5 y/M	No lesion	Normal	High ADC	No lesion	No lesion
5 y/F	No lesion	Normal	High ADC	No lesion	No lesion

Note.—In all patients, FLAIR images showed cerebellar hyperintensity.

cerebellum, an elevated diffusion pattern was predominant in the five juvenile cases, and a restricted diffusion pattern was evident in an infantile case. In the cerebrum of the two juvenile cases and the infantile case, a restricted diffusion pattern was noted in the lesions. In one juvenile case, the lesions had an elevated diffusion pattern. These findings likely represent different histopathologic stages in neuroaxonal dystrophy.

### References

1. Farina L, Nardocci N, Bruzzone MG, et al. **Infantile neuroaxonal dystrophy: neuroradiological studies in 11 patients.** *Neuroradiology* 1999;41:376–380
2. Nardocci N, Zorzi G, Farina L, et al. **Infantile neuroaxonal dystrophy: clinical spectrum and diagnostic criteria.** *Neurology* 1999;22;52:1472–1478
3. Simonati A, Trevisan C, Salviati A, Rizzuto N. **Neuroaxonal dystrophy with dystonia and pallidal involvement.** *Neuropediatrics* 1999;30:151–154
4. Rodriguez Costa T, Cabello A, Recuero-Fernandez E, et al. **Infantile neuroaxonal dystrophy: a report of two new cases and a review of the literature published over the past ten years.** *Rev Neurol* 2001;33:443–447
5. Santucci M, Ambrosetto G, Scaduto MC, Morbin M, Tzolas EV, Rossi PG. **Ictal and nonictal paroxysmal events in infantile neuroaxonal dystrophy: polygraphic study of a case.** *Epilepsia* 2001;42:1074–1077
6. Friede RL. *Developmental Neuropathology*. 2nd ed. Berlin: Springer-Verlag; 1989:555
7. Sener RN. **Diffusion magnetic resonance imaging in infantile neuroaxonal dystrophy.** *J Comput Assist Tomogr* 2003;27:34–37